Effects of surface flow visualisation on aerodynamic loads at low Reynolds number

L. W. Traub
traubl@erau.edu
R. Waghela and E. M. Botero
Aerospace and Mechanical Engineering Department
Embry-Riddle Aeronautical University
Prescott
USA

ABSTRACT

In this article, the effect of on-surface flow visualisation (SVF) techniques on measured loads over an airfoil are explored. Titanium dioxide based mixture effects on the lift and drag coefficient are experimentally quantified at low Reynolds numbers by recording the time history as the patterns evolve and freeze. With statistical comparison based on Student's *t*-distribution method, it was determined that the effect on the drag coefficient was minimal but the lift coefficient was slightly attenuated. Additionally, it was observed that at high angles-of-attack the temporal history of the flow as the wind tunnel ramps up may alter the steady-state flow field in the presence of a SFV mixture.

Paper No. 4246. Manuscript received 12 August 2014, revised version received 8 December 2014, accepted 9 December 2014.

https://doi.org/10.1017/S0001924000010745 Published online by Cambridge University Press

1.0 INTRODUCTION

Surface flow visualisation (SFV) is a diagnostic technique commonly used for the clarification of fluid flow physics. SFV can be used to investigate stagnation point locations, separation lines, locations of boundary layer transition, vortical flows, extent of separation zones, and critical points (nodes, saddles etc.)[1-2]. Tufts and various oil mixtures are commonly used SFV techniques.

Oils and pigments/dyes used for SFV are combined to form a mixture such that airflow can exert sufficient shear stress to form a discernable flow pattern but not readily flow under the influence of gravity. The choice of oils and pigment/dye is generally determined according to the airspeed and is usually painted or sprayed on the area of interest. When exposed to airflow, the mixture flows due to shear stress from the airstream, pressure gradients, and gravitational forces[1,3]. The streaky deposit of the pigment provides clues regarding direction of the flow. Different streak patterns result for laminar and turbulent flow within the boundary layer[4].

Researchers have speculated regarding the reliability of observations based on SFV derived patterns as the mixture affects the boundary conditions for the airflow[4]. Squire[3] provides an analytical analysis of the interaction between a SFV mixture and airflow. Squire's work shows that mixture flow depends on the shear stress (skin friction) due to the airflow and on the pressure gradients. Usually, the pressure term is much smaller compared to the skin friction, and the streak pattern forms a reasonable representation of the actual limiting streamlines. If the pressure gradient is large, such as near separation or reattachment lines, mixture flow is decelerated and film thickness increases, which can contribute to altering the location of apparent flow separation or reattachment.

Barlow *et al*[1] provide some experimental evidence that SFV techniques, including tufts and china clay-oil mixtures, affect aerodynamic loads. Their data[1] shows a moderate decrease in the maximum lift coefficient with varying sensitivity to china clay and different types of tufts. The data presented is for the high angle-of-attack regime over a generic transport style wing. The test Reynolds number was not specified. Data was not included regarding effects on drag. Additionally, the differences in aerodynamic loads are relatively small; the uncertainty bounds of the measuring equipment used was not indicated.

Surface flow patterns evolve with time until frozen due to drying or until a steady state has been achieved. As the surface patterns evolve with time, changes in aerodynamic loads may occur. A survey of the literature did not reveal information regarding the variation in aerodynamic forces during this unsteady period or once steady state has been achieved. For high Reynolds number testing, such considerations may be moot. In the low Re regime typical of small unmanned aerial vehicles, clarification is required on the effects of surface diagnostic techniques on load evolution. Specifically whether the use of SFV may alter the flow physics such that they are no longer representative of that on the clean airfoil/wing. Consequently, does an observed surface pattern correlate with measured force balance data at similar conditions.

This study aims to quantify the effect of a SFV mixture consisting of titanium dioxide, linseed oil, and kerosene. The focus of this study is to measure effects on the lift and drag coefficient at Reynolds numbers of 100,000 and 150,000 (which are representative for a small unmanned aerial vehicle). Uncertainty analysis is conducted using Student's *t*-distribution to distinguish between the uncertainty from the apparatus and trends in the data. The scope of this study is limited to the aerodynamic load variations after the wind tunnel achieved test speed until the SFV pattern froze. The effects of SFV mixture are investigated at three different angles of-attack (α), 4°, 12°, and 16°.

https://doi.org/10.1017/S0001924000010745 Published online by Cambridge University Press

2.0 EQUIPMENT AND PROCEDURE

Wind tunnel testing was conducted in Embry-Riddle Aeronautical University's 1 by 1ft open-return-tunnel. This facility has a measured turbulence intensity of 0·25% and velocity uniformity greater than 99%. The force measurements were conducted using an external three-component platform balance with a load range of 45 Newtons for lift and drag. The load cell voltages are digitised using a National Instruments 14-bit A/D board. The angle-of-attack was set using a Velmex stepper motor controller yielding repeatability within 0·1 degrees. This balance supports the model in a vertical orientation to eliminate any effects of center of gravity shift. Data acquisition, processing and recording is accomplished with a LabVIEW interface. The data acquisition uses a Butterworth low-pass filter set at 20Hz for all inputs. All presented data points represent 1,000 averages. The uncertainty of the force-balance used for this experiment was approximately 0·001 for coefficients of lift and drag.

A Selig S8036 airfoil section wind tunnel model was designed using CATIA and was manufactured using a Stratasys 768 SST three-dimensional rapid prototyping printer yielding a model composed of acrlylonitrile butadiene styrene (ABS) plastic. This model was designed to fit both the force balance and a rotatable wall plug to allow mounting in vertical and horizontal orientations. The model's chord was 99·1mm and the span 303·2mm. Clearance between the model and the walls of the tunnel was 0·6mm-0·8mm.The airfoil's trailing-edge was 0·2mm thick. Two sets of wind-tunnel tests were conducted at Re = 100,000 and 150,000. The first set of data was collected to establish repeatability. The second data set was used to determine the uncertainty intervals of the aerodynamic loads and the effects of flow visualisation. For the first set of data, multiple angle-of-attack sweeps were performed from –4° to 18° in 2° increments without application of the SFV mixture.

For the second set of data, the model was set to a desired angle-of-attack after which several data points were taken. Data was collected at 4°, 12°, and 16° angle-of-attack, representing the attached flow pre- and post-stall regimes. At least 12 data points were taken at each incidence. The Student's *t*-distribution was used to determine uncertainty intervals[5] as the *t*-distribution is effective for small sample sizes[5]. The intervals were determined to a confidence level of 99 percent. The uncertainty interval was estimated using[5].

$$\Delta Coefficient = \frac{t\sigma}{\sqrt{n}} \qquad \ldots (1)$$

where t is the confidence level, σ is the standard deviation and n is the number of readings. The standard deviation of the mean is given by $\sigma/(n^{0.5})$. From tables[5], $t = 3{\cdot}106$ for 12 readings (11 degrees-of-freedom).

After the repeated data measurements, the SFV mixture was painted on the upper surface of the wing and the wind tunnel was switched on. When the wind tunnel achieved the test speed, quantitative (force-balance) and qualitative (photographs) data were taken at approximately 3-4 second intervals until the pattern was frozen. This process was repeated for additional data after cleaning the wing but without altering the position of the wing; performing repeat tests without altering model position eliminates any variability in angle-of-attack.

The viscosity of the SFV mixture was estimated using the Refutas Equation[6]. The viscosity blending number for the constituents; linseed oil and kerosene was calculated as well as the viscosity blending number of the mixture. Finally, the kinematic viscosity of the blend was then estimated[6] as 2·89cSt. The thickness of the oil film was estimated to be ≈ 0·1mm.

https://doi.org/10.1017/S0001924000010745 Published online by Cambridge University Press

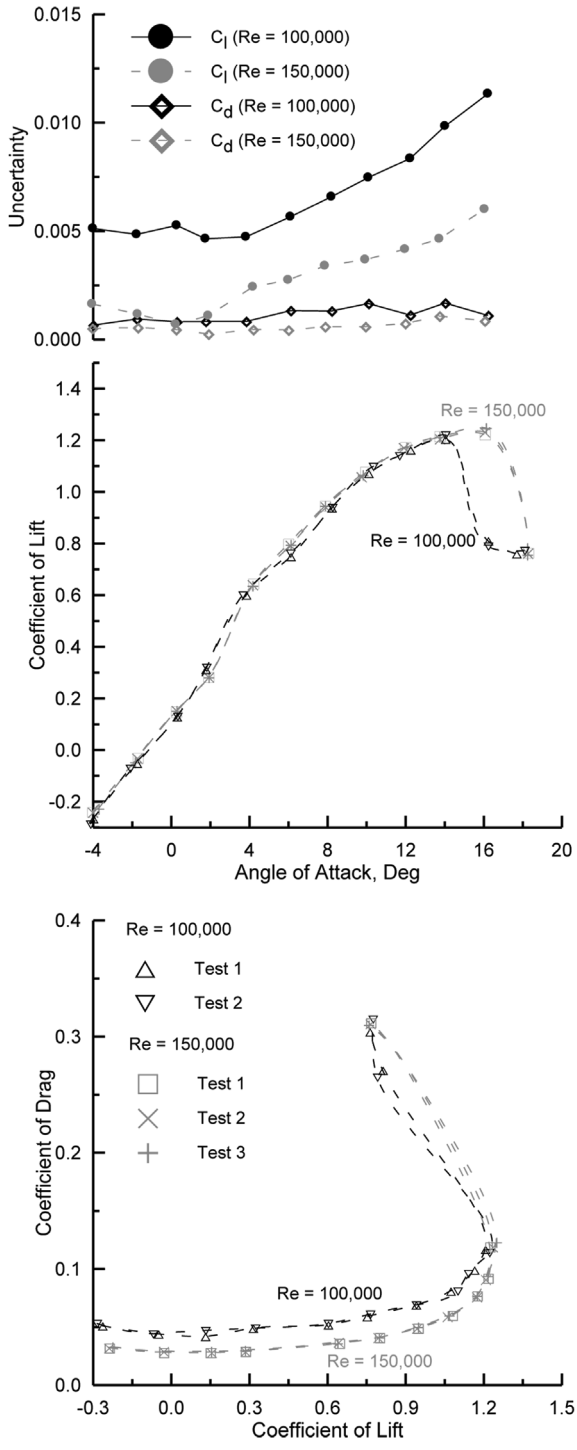


Figure 1. Repeated data runs and 99% uncertainty intervals.

https://doi.org/10.1017/S0001924000010745 Published online by Cambridge University Press

4.0 RESULTS AND DISCUSSION

Figure 1 shows a quantification of the ability of the wind tunnel balance to reproduce data runs. The plot contains repeat data for the lift curve and drag polar of the S8036 airfoil at 100,000 and 150,000 Reynolds numbers. The results in Fig. 1 shows excellent repeatability. The lift curve shows low Reynolds number traits. The non-linearity in the lift curves is caused by the presence and movement of a laminar separation bubble on the upper surface of the wing, as well as induced camber from boundary layer displacement thickness effects[7]. The increase in Reynolds number causes a moderate increase in the maximum coefficient of lift and a delay of the stall angle. The drag polar also shows Reynolds number effects. The minimum coefficient of drag for Re = 100,000 shows an increase (primarily skin friction) compared to Re = 150,000 that is associated with a lowering of Reynolds number. Drag data is repeatable throughout the domain of this investigation.

Figure 1, top plot, shows the uncertainties for the coefficients of lift and drag as a function of angle-of-attack. The uncertainty was calculated using repeated data and Student's *t*-distribution. The effect of the SFV mixture on the lift and drag coefficient is shown in Figs 2 and 3 for Reynolds numbers of 100,000 and 150,000, respectively. Included in these figures are inset images showing SFV renderings of the surface flow. The period T is that at which the surface pattern was observed to be 'frozen'; t represents time.

The experimental data was collected at 4°, 12°, and 16° angles-of-attack. These angles-of-attack capture unique flow regimes. At 4° angle-of-attack the flow is primarily attached but a laminar separation bubble is present, at 12° there are regions of attached and separated flow, and at 16° there are large regions of separated flow.

At 4° angle-of-attack, the data in Fig. 3 shows a time lag in achieving a lift coefficient within the uncertainty interval for Re = 150,000. This result indicates that the SFV mixture interacts with the airflow such that the lift force is attenuated. As the pattern freezes, the aerodynamic coefficients approach that of the clean configuration. The inset flow visualisation images clearly show a delay in the formation of the laminar separation bubble. The lag is associated with the location of separation which moves aft with t/T (contracting the bubble), not to the location of flow re-attachment, shown clearly in Fig. 3. For Re = 100,000, Fig. 2, the data appears to fall within the uncertainty interval.

At 12° angle-of-attack, the mix of attached and separated flow causes significantly larger variation in loads; even for the clean wing as seen by larger uncertainty intervals. At both Re, the surface patterns show a separation bubble close to the leading edge followed by a run of turbulent flow that terminates in trailing-edge separation. At Re = 100,000, the data shows dispersion about the uncertainty interval suggesting that the presence and movement of the fluid affects the imposed loads. At Re = 150,000, the inset images show a clear delay in the visualisation of the trailing-edge separation. Indicated lift appears slightly below the uncertainty interval for the clean wing with moderate dispersion.

At 16° angle-of-attack, the trends for 100,000 and 150,000 Reynolds number are significantly different. At a Reynolds number of 100,000, the variation of loads is similar to 4 or 12°. Initially, the data demonstrates a significant amount of scatter which attenuates with time to fall approximately within the lower bound of the uncertainty interval. The scatter is significantly greater than at 4 or 12°, a consequence of the unsteadiness of separation. At Re = 150,000, the data shows a bifurcation, such that the flow appears to switch between two equilibrium states. After achieving the test Re, the loads are indicative of those post stall, Fig. 1. The surface flow was then observed to rapidly show the onset of flow re-attachment manifest in a significant increase in the lift coefficient and a reduction in the drag coefficient. The inset images initially show massive separation ($t/T < 0{\cdot}3$),

https://doi.org/10.1017/S0001924000010745 Published online by Cambridge University Press

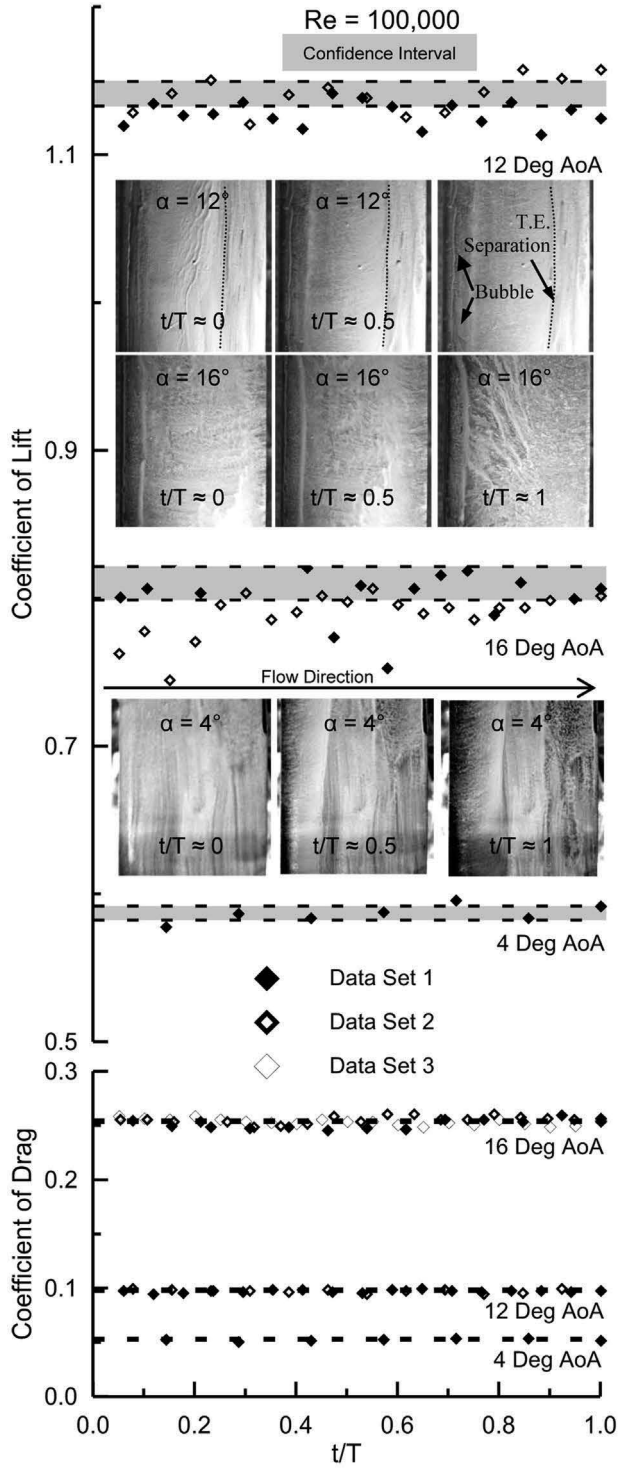


Figure 2. Effect of SFV on temporal evolution of lift and drag coefficient, Re = 100,000.

https://doi.org/10.1017/S0001924000010745 Published online by Cambridge University Press

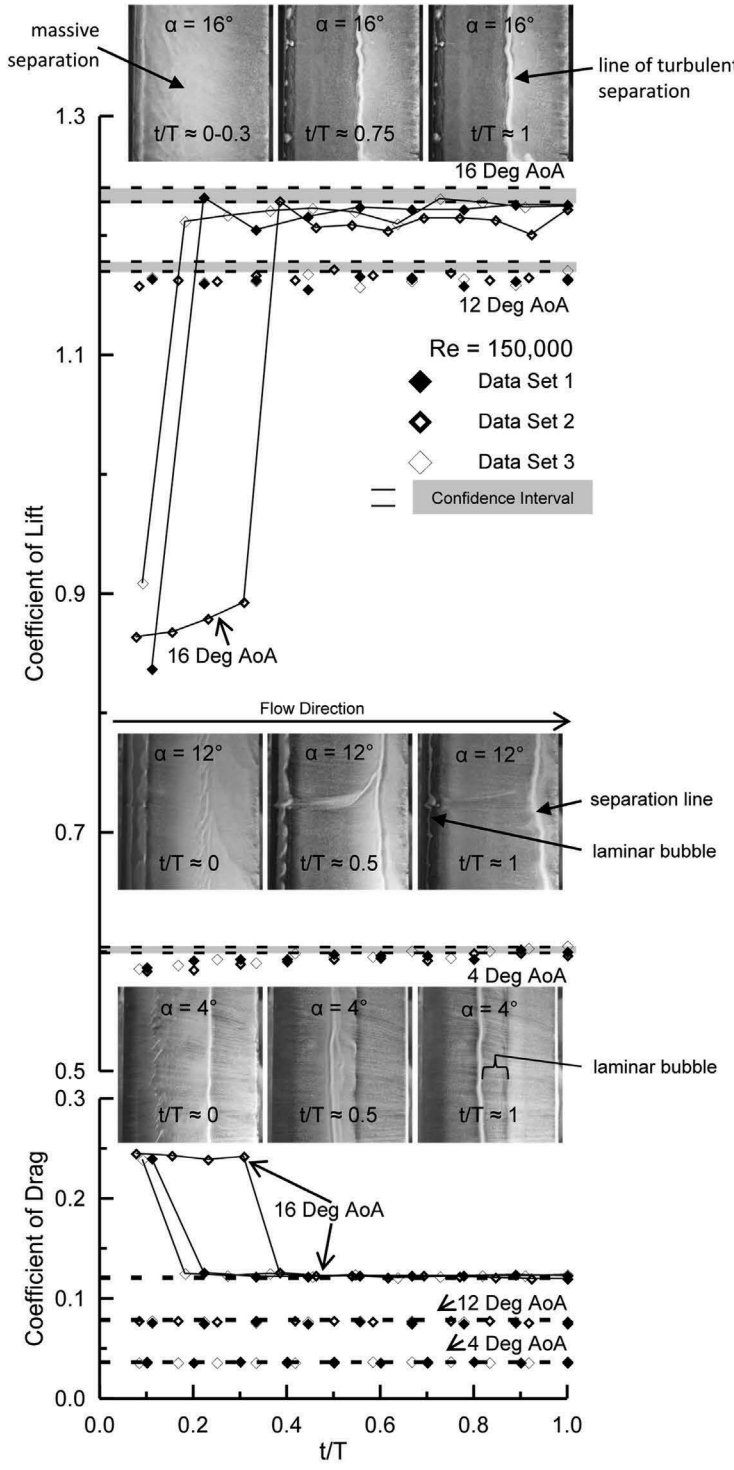


Figure 3. Effect of SFV on temporal evolution of lift and drag coefficient, Re = 150,000.

https://doi.org/10.1017/S0001924000010745 Published online by Cambridge University Press

followed by re-attachment yielding trailing-edge separation from approximately the mid-chord aft ($t/T > 0{\cdot}3$). As observed for lower incidence, the 'frozen' (time invariant) lift coefficient is slightly below that of the clean loading case (i.e. below the gray uncertainty interval). The bifurcation in the flow may stem from two effects. The first effect is associated with the impact of the SFV medium itself. Increasing Re yields a net reduction in boundary layer thickness. Consequently, at higher Re the reduction in boundary layer thickness may render the surface paint as capable of acting as a widely distributed surface trip. The second effect is the time lag associated with acceleration of the flow to the set Re. As may be observed in Fig. 1, lower Re reduces the stall angle. Thus the fluidic history of the wing is established as the Re number increases from zero. At low Re the flow would be separated and may-reattach as the Re increases such that transition of the laminar shear layer is achieved. This would culminate in a closed laminar separation bubble at the leading edge location. The bifurcation seen in Fig. 3 was not evident in testing without SFV. With reference to Fig. 1, $\alpha = 16°$ corresponds to a similar lift coefficient (approximately the maximum lift coefficient) to that seen in Fig. 3 with the SFV mixture applied. Setting the wing at 16° incidence (without the SFV mixture) and starting the tunnel yielded a final lift coefficient of approximately 0·85, or that seen initially ($t/T > 0{\cdot}3$) in Fig. 3. Consequently if the wing incidence is increased from an initially attached flow regime, the outcome may be different to starting the wing at high incidence, where the Re history of the flow manifests in the steady state loads. In Fig. 3, the application of SFV 'fortuitously' promotes transition such that equivalent loading to that seen in Fig. 1 is achieved. Consequently, it may be inferred that a more reliable approach would be to apply the SFV, start the tunnel and then bring the wing to the desired α. This can be problematic though, as the pattern may 'freeze' at a non-representative incidence.

The application of the SFV mixture shows little impact on the drag coefficient at Re = 150,000. In contrast, fluctuations around the uncertainty interval at Re = 100,000 and $\alpha = 16°$ are seen to be significant. The coefficient of drag shown in Fig. 2 and Fig. 3 is approximately time invariant. Taken as a whole, the close accord in the measured lift and drag coefficients with and without SFV implies that the surface skin friction patterns are indeed representative of those over the clean wing.

The force balance measurements and SFV application were conducted with the wing mounted vertically. The impact of gravity on the behavior of the liquid SFV medium was examined through tests with the wing in a horizontal orientation. Images are presented in Fig. 4 with a summary in Table 1. As seen, the dominant flow features comprising the leading edge separation bubble and line of trailing-edge separation are little affected by the wing orientation. Thus, the SFV images in Figs 2 and 3 may be regarded as representative of those for the section positioned horizontally.

Table 1
Effect of wing orientation on separation and attachment locations

Flow Feature	Horizontal Mount – Extent Position (% Chord)*	Horizontal Mount – Extent Position (% Chord)*
Attached Laminar Flow ($\alpha = 12°$)	96-100	96-100
Laminar Separation Bubble ($\alpha = 12°$)	82-96	82-96
Attached Turbulent Flow ($\alpha = 12°$)	25-82	25-82
Separated Flow ($\alpha = 12°$)	0-25	0-25
Laminar Separation Bubble ($\alpha = 16°$)	81-98	82-96

***Extent measured from trailing-edge.**

https://doi.org/10.1017/S0001924000010745 Published online by Cambridge University Press

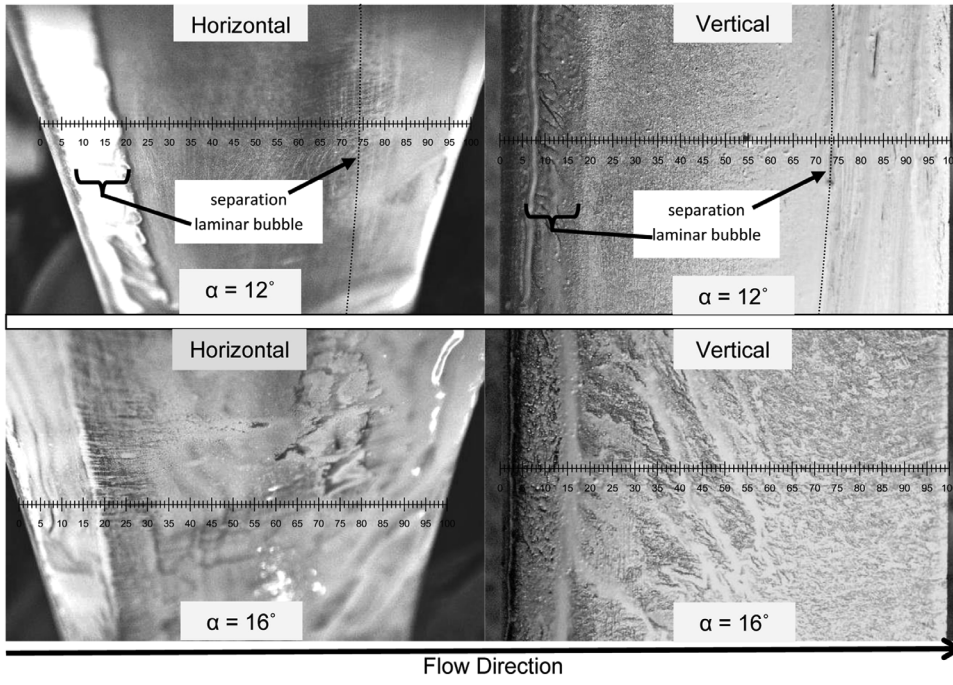


Figure 4. Effect of wing orientation on rendered surface flow patterns. Flow from left to right.

CONCLUSIONS

An experimental investigation was conducted to ascertain the effect of surface flow visualisation on aerodynamic loads at low Re number. The lift and drag coefficient of a S8036 airfoil were measured at Re = 100,000 and 150,000. Tests were repeated to establish uncertainty intervals such that the significance of the measurements could be established. The data indicated little effect of the surface paint mixture on the drag coefficient, while the lift coefficient showed a slight attenuation compared to that recorded without surface paint. Based on the observed loading equivalence between the clean wing and that coated with the surface flow visualisation medium, it may be surmised that the skin friction topology was representative of that over the clean wing. In certain instances, it was observed that the temporal history of the flow as the wind tunnel velocity ramps up may alter the final flow field at steady state. In this instance, the presence of a surface paint may alter the outcome.

ACKNOWLEDGEMENT

The authors would like to acknowledge the support of Rajmohan Waghela and Emilio Botero through an Embry Riddle Aeronautical University IGNITE undergraduate research grant.

https://doi.org/10.1017/S0001924000010745 Published online by Cambridge University Press

REFERENCES

1. BARLOW, J.B., RAE, W.H. and POPE, A. *Low-Speed Wind Tunnel Testing*, 3rd ed, John Wiley & Sons, New York, NY, USA, 1999, pp 192-205.
2. SETTLES, G.S. *Aerospace and wind tunnel testing*, Handbook of flow visualization, Wen-Jei Yang, 2nd ed, Francis & Taylor, New York, NY, USA, 2001, pp 395-408
3. SQUIRE, L.C. The motion of a thin oil sheet under the steady boundary layer on a body, *J Fluid Mechanics*, 1961, **11**, (2), pp 161-179.
4. MERZKIRCH, W. *Flow Visualization*, Academic Press, Orlando, FL, USA, 1987, pp 82-89.
5. HOLMAN, J.P. *Experimental Methods for Engineers*, 8th ed, New York, NY, USA, McGraw Hill, 2012, pp 112-116.
6. MAPLES, R.E. *Petroleum refinery process economics*, PennWell, 2nd ed, 2000.
7. TRAUB, L.W. and FREIENMUTH, E. Effect of streamwise attachment gap on aerodynamic characteristics of gurney flaps, *J Aircraft*, 2011, **48**, (1), pp 348-351.

https://doi.org/10.1017/S0001924000010745 Published online by Cambridge University Press